nature photonics

SUPPLEMENTARY INFORMATION

DOI: 10.1038/NPHOTON.2016.36

# Broadband dispersion-engineered microresonator on a chip

## I. DISPERSION PARAMETERS FITTING

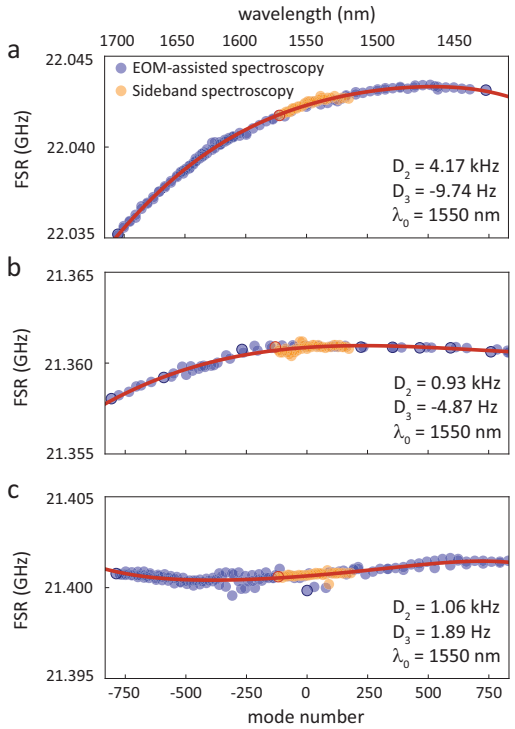


FIG. S1: **Dispersion parameters fitting** (**a**) Measured FSR of single-wedge disk and the Taylor series fit (solid line). Blue dots represent the measurement value using the EOM comb method (Fig. 3a), and red dots are measured by sideband spectroscopy[S1,S2] for comparison. The FSR is 22.042 GHz at 1550 nm. (**b-c**) Same as panel **a**, but for quadruple-wedge disks. FSR: 21.36 GHz for (**b**), 21.40 GHz for (**c**) at 1550 nm.

The resonance frequencies of one mode family can be described as a Taylor series shown in eqn.(2), and the coefficients of the series correspond to dispersion parameters at $\mu = 0$. The FSR can also be expressed as a Taylor series with the same coefficients in eqn.(2).

$$FSR(\mu) = D_1 + D_2 \cdot \mu + \frac{D_3}{2!}\mu^2 + \cdots \qquad \text{(S1)}$$

Fig. S1 shows the measured FSR of single- and quadruple-wedge structures (Fig.3), and the fitted polynomial curves (eqn.(S1)) to the experimental results. Here, FSR was measured using both EOM-assisted (Fig. 3a, 300-nm-bandwidth) and sideband[S1] (70-nm-bandwidth) spectroscopy methods. $\Delta$FSR per mode ($D_2$) is relatively small (<10 kHz /mode), thus it is necessary to accumulate the change of FSR throughout multiple mode numbers ($\mu$) in order to perform the fitting.[S1].

## II. CONFIDENCE IN SEM/ AFM-BASED DISPERSION CALCULATION

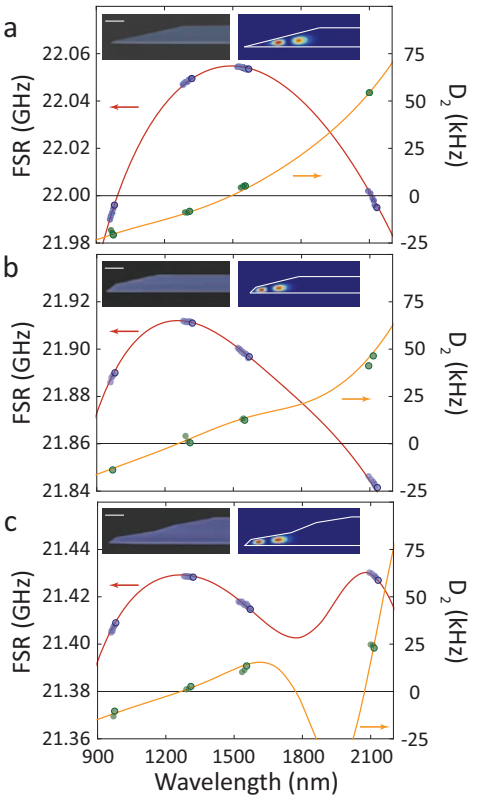


FIG. S2: **Dispersion in higher-order mode** TM1 mode FSR and $D_2$ for **(a)** single-, **(b)** double-, **(c)** quadruple-wedge disks shown in Fig. 3. The dots are from the measurement and solid lines are numerically calculated FSR (Red) and $D_2$ (Orange) from the same resonator structure. Insets show SEM images of resonator and the simulated TM1 mode profile.

The finite-element-simulation calculates the resonance frequencies (eqn.(2)) based on AFM and SEM measurements. Generally, the structural parameters from the microscope measurement are finely tuned within a range of $\pm$ 0.5 % of the measured parameters in order to obtain a good fitting, and the tuning might correct the uncertainty of resonator profile measurements.

The measurement of higher-order mode dispersion can provide additional confidence in the connecting resonator structure and dispersion. Fig. S2 shows the measured FSR, $D_2$ of the TM1 mode (see insets for mode profile), and the results of simulations from the geometry in Fig. 3. Here, the structural parameters are exactly same with those for fundamental mode calculations (i.e., no extra tuning of the structure to fit

DOI: 10.1038/NPHOTON.2016.36

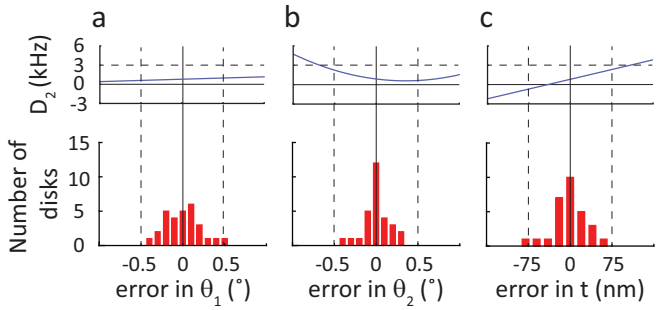


FIG. S3: **Reproducibility of resonator fabrication** Structural parameter variations and simulated impact on $D_2$ for **(a)** $\theta_1$ (outer wedge angle), **(b)** $\theta_2$ (inner wedge angle), and **(c)** t (outer wedge height) of the double-wedge disk. Structural parameters were measured from fabricated double-wedge disks with the same design as the one in Fig. 3c, and $D_2$ is calculated as a function of one of the parameters while other parameters are fixed.

the TM1 dispersion).

The imprecision of micro-fabrication[S3,S4] might lower the repeatability of dispersion in fabricated disks. It can also impact the repeatability of resonator geometry design to achieve specifed dispersion coefficients. As a preliminary test of process accuracy, double-wedge disks (29 EA) were identically fabricated from multiple wafers (4 EA) and structural parameters were measured using an AFM (see Fig. S3). The measurements show 30.4 nm, 0.21°, and 0.15° standard deviations in t, $\theta_1$, and $\theta_2$, respectively(actual values are 2.92 $\mu$m, 43.5°, and 10.5° for t, $\theta_1$, and $\theta_2$). In order to understand how this imprecision in the process impacts the dispersion of the resonator, we have run a set of simulations on double-wedge disks and independently varied t and $\theta_{1,2}$ by ± 150 nm and 1°, respectively. Based on numerical simulation, the standard deviations of t, $\theta_1$, and $\theta_2$ approximately cause 0.8, 0.01, 0.3 kHz of $D_2$ variations from the designed dispersion parameter, respectively. For simplicity, $D_2$ variation was calculated as function of a single parameter (one of t, $\theta_1$, and $\theta_2$) assuming other geometric parameters constant.

[S1] Li, J., Lee, H., Yang, K. Y. & Vahala, K. J. Sideband spectroscopy and dispersion measurement in microcavities. *Opt. Express* **20**, 26337–26344 (2012).

[S2] Del'Haye, P., Beha, K., Papp, S. B. & Diddams, S. A. Self-injection locking and phase-locked states in microresonator-based optical frequency combs. *Phys. Rev. Lett.* **112**, 043905 (2014).

[S3] Lee, H. *et al.* Chemically etched, ulta-high-Q resonator on a chip. *Nature Photon.* **6**, 369–373 (2012).

[S4] Kordts, A., Pfeiffer, M. H. P., Guo, H., Brasch, V. & Kippenberg, T. J. Higher order mode suppression in high-q anomalous dispersion sin microresonators for temporal dissipative kerr soliton formation. *Opt. Lett.* **41**, 452–455 (2016).